2

A CHARACTERISTIC OF CRANKSHAFT BEHAVIOUR AT THE INITIAL FIRING STAGE

Aminudin Hj Abu
Oh, Jae-Eung
Lee, Jung-Youn

2.0 INTRODUCTION

The demands on a modern engine system are increasing rapidly. High performance engines, low fuel consumption, low noise and vibration are several factors that a customer demands simultaneously. These demands pressurise engineers to upgrade engine designs and require optimisation of engine components.
Since the crankshaft is one of the key components in the engine system, identification of dynamic behaviour plays an important role in the design. Thus, an accurate prediction for the dynamic characteristics of the system using finite element method is essential for modern equipment.

The crankshaft, supported by the crankcase bearing, receives the combustion gas force and gas torque force exerted from the pistons through the connecting rod in each cycle. These gas forces are due to the gas from the exploding fuel air mixture impinging on top of the piston surface while the gas torque is due to the gas force acting at the moment arm about the crankshaft center. Generally, the latter forces are higher and act cyclically.

Therefore, one must study the behaviour and characteristics and, finally, identify the dominant forces in each frequency domain,

whereby the equations of motion of the system are expressed in terms of frequency and integrated in the frequency domain to obtain the frequency response. The advantage of this method is the high frequency components of the systems can be eliminated and the computation can be reduced. Also, interpretation of the results is simpler than the 'time history' solution. For nonlinear equations, a sinusoidal random input describing function approach could be used.

Previous crankshaft analyses were based on modal analyses and experiments [1][2][3] and were not given a detailed explanation. There is a need to contrast more especially the involvement with the operating stage. Consideration of the load history in time domain [4] under the running conditions is obviously important but the high frequency components of the system cannot be eliminated since the range of time domain is not limited. The analysis using rotating coordinate system [5] under operating conditions, investigated at the initial firing, with consideration of several cases dealing with the pulley and flywheel, may be obtained by instructive knowledge about the behaviour. But, in this chapter the bending by dynamic behaviour modes, affected mainly at the bearing journal, is preferable since journal bearings are the most sensitive section to be considered since they receive a repetitive load history.

As new engines are continuously researched and developed, a design process is required from the beginning of the engine design stages, and engine designers need to know the precise vibration behaviour of the crankshaft system. For these needs, a simple modelling method and computation approach for the crankshaft system [6] has been reported. The modelling and analyses of crankshaft vibrations in the frequency domain including the effects of the rotation of the crankshaft under operating conditions are given in reference [5].

This chapter describes a new method of analysis of the dynamic behaviour of the crankshaft vibrations in the frequency domain based on initial firing stage where the force is given at the first crankpin. The new method includes the effect of Root Mean

Square (RMS) value for the calculated energy at each bearing journal under the firing conditions. There are three main objectives of this chapter. Firstly, to verify the highest load case under the firing stage. Secondly, to identify the response at journal bearing location using RMS value, and finally, to estimate the transferable energy corresponding to the modifying counter weight. The modifications of counter weights are based on an assumed shape where the RMS value has been investigated during modal analysis diagnostics.

2.1 Modelling of the crankshaft

A crankshaft system is one of the most complex structure systems. Therefore, the crankshaft system used in this chapter is being simplified as much as possible without violating the originality of the system towards vibration analysis. In the case of modal analysis, the crankshaft was idealised by a set of jointed structures consisting of round and blocks of rectangular beam cross-sections. In order to simplify the analysis, pin and arm parts are assumed to have uniform section. In the case of total engine, the flywheel, bearing journals, and pulley are taken into account. Details of the modelling method can be summarised as follows; Since the flywheel is relatively thin, the flywheel is idealised by triangular plate elements. However, the original mass and the moment of inertia of the flywheel is preserved in the x, y and z directions since the flywheel has sufficient rigidity in these directions. The reciprocating masses consist of the masses of the pistons and the mass of the small end in the connecting rod are attached at the crankpin end. The crank journal bearings are idealised by three set of linear springs and dashpots in the y and z directions. The front pulley and the crank gear are idealised by a set of lumped masses and moment inertia attached at their centers of gravity. The engine block is idealised by a rigid body supported with linear springs in x, y and z directions to the ground. The

stiffness is used from the data given in the previous report by Khang [7]. The idealised crankshaft model is shown in Figure 2.1 and the idealised engine model is shown in Figure 2.2

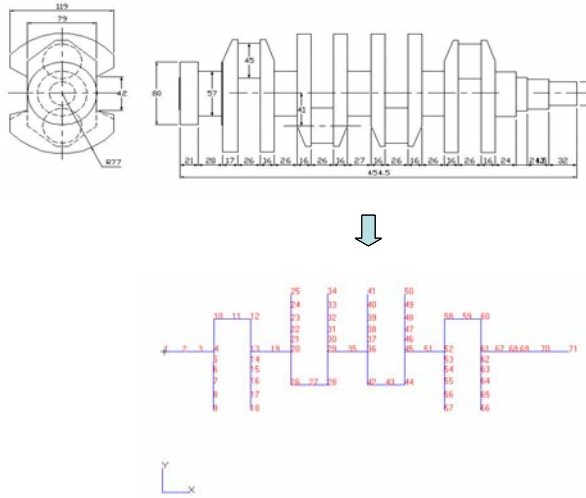

Figure 2.1 Idealised model of the crankshaft

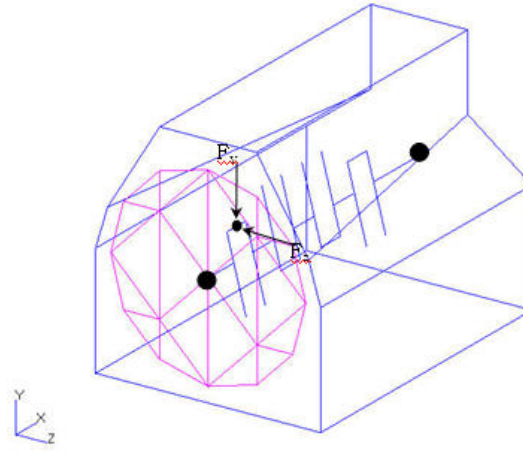

Figure 2.2 Idealised model of the crankshaft with the engine

1.2.1 THEORY

2.1.1 Equation of Motion

The crankshaft system may be presented by a sum of the n dividable finite elements. Figure 2.3 shows the node points of an element e. Each node point has six degrees of freedom which consist of three linear displacements υ_x, v_y, w_z and three rotational displacements $\theta_x, \theta_y, \theta_z$, and can be presented by

$$\{\mathbf{u}\}_e = \{\upsilon_{x1}, v_{y1}, w_{y1}, \theta_{x1}, \theta_{x1}, \theta_{z1}, \upsilon_{x2}, v_{y2}, w_{z2}, \theta_{x2}, \theta_{y2}, \theta_{z2}\} \quad (1)$$

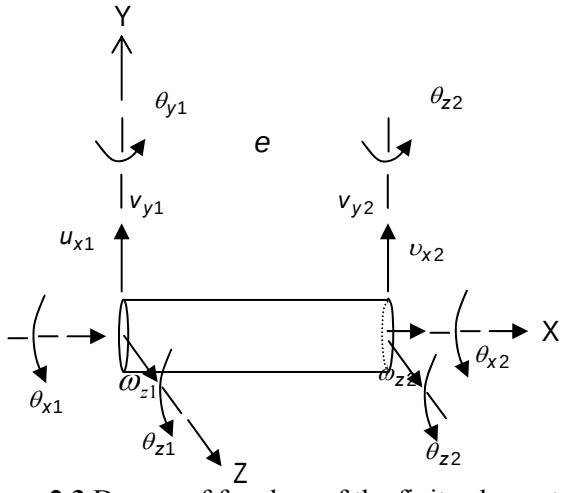

Figure 2.3 Degree of freedom of the finite element

The kinetic energy for n degrees of freedom system can be expressed as

$$KE_e = \frac{1}{2}\int \{\dot{\mathbf{u}}\}^{\mathbf{T}} \{\dot{\mathbf{u}}\}\rho\, dv \tag{2}$$

where;

ρ - density (mass per unit volume)

$\{\dot{\mathbf{u}}\}$ - velocity vector

In the finite element, the system is divided into elements and each element of the displacement vector $\{\mathbf{u}\}$ is expressed in terms of the nodal displacements $\{\mathbf{q}\}$, using shape the function **N**. However, in dynamic analysis, the elements $\{\mathbf{q}\}$ are dependent on time, while **N** represents the shape function defined on a master element where the velocity vector is the given by

$$\{\dot{\mathbf{u}}\} = \mathbf{N}\{\dot{\mathbf{q}}\} \tag{3}$$

Substituting equation (3) into equation (2), the kinetic energy in element e is

$$KE_e = \frac{1}{2}\{\dot{\mathbf{q}}\}^{\mathbf{T}}\left[\int_e \rho \mathbf{N}^{\mathbf{T}}\mathbf{N}dv\right]\{\dot{\mathbf{q}}\} \tag{4}$$

where the bracketed term denotes the element mass matrix

$$\mathbf{m_e} = \int_e \rho \mathbf{N}^{\mathbf{T}}\mathbf{N}dv \tag{5}$$

Thus, the element kinetic energy can be written as

$$KE_e = \frac{1}{2}\{\dot{\mathbf{q}}\}_{\mathbf{e}}^{\mathbf{T}}\mathbf{m_e}\{\dot{\mathbf{q}}\} \tag{6}$$

The strain energy term is considered when obtaining the stiffness matrix. The strain energy for an element is

$$U_e = \frac{1}{2}\int_e \{\sigma\}^T \varepsilon A dx \tag{7}$$

for $\sigma = E\mathbf{B}\{\mathbf{q}\}$ and $\varepsilon = \mathbf{B}\{\mathbf{q}\}$, where

σ - stress in terms of nodal value
ε - strain in terms of nodal value
$\mathbf{B}$ - element strain-displacement matrix
E - Young's modulus

Thus

$$\begin{aligned} U_e &= \frac{1}{2}\int \{\mathbf{q}\}^{\mathbf{T}} [\mathbf{B}]^{\mathbf{T}} E[\mathbf{B}]\{\mathbf{q}\} A dx \\ &= \frac{1}{2}\{q\}^T \left[\int_e [\mathbf{B}]^{\mathbf{T}} E[\mathbf{B}] A dx\right]\{\mathbf{q}\} \end{aligned} \tag{8}$$

The bracketed term shows the stiffness element

$$\mathbf{k_e} = \int_e [\mathbf{B}]^{\mathbf{T}} E[\mathbf{B}] A dx \tag{9}$$

Thus, the potential energy, PE of elastic system in finite element method can be expressed as

$$PE = \frac{1}{2}\{\mathbf{q}\}_{\mathbf{e}}^{\mathbf{T}} \mathbf{k_e} \{\mathbf{q}\}_{\mathbf{e}} - \{\mathbf{q}\}_{\mathbf{e}}^{\mathbf{T}} \{\mathbf{f_e}\} \tag{10}$$

Using the Lagrangian, $L = KE - PE$, the equations of motion are obtained without consideration of damping as

$$\mathbf{m}_e \{\ddot{\mathbf{q}}\}_e + \mathbf{k}_e \{\mathbf{q}\}_e = \{\mathbf{f}\}_e \tag{11}$$

If a damping is considered, the equations of motion in equation (11) can be rewritten as

$$\mathbf{m}_e \{\ddot{\mathbf{q}}\}_e + \mathbf{c}_e \{\dot{\mathbf{q}}\} + \mathbf{k}_e \{\mathbf{q}\}_e = \{\mathbf{f}\}_e \tag{12}$$

2.1.2 Background of a Single Crankshaft

This section serves as a general background in understanding the generation of shaking vibration in a reciprocating machine. Figure 2.4 shows a free body diagram of a single crank mechanism. $\boldsymbol{F_g}$ is the gas force vector acting on the piston center, where the magnitude is $\boldsymbol{F_g}=\pi D^2 P_g/4$, where P_g is gas pressure and D is the bore cylinder. $\boldsymbol{F_a}$ is the horizontal reactive gas force of the piston on the cylinder wall and the distance *x*, which is the instantaneous moment arm of O. The force trying to rock the ground plane is called the reaction gas torque, $\boldsymbol{F_{sy}}$ and $\boldsymbol{F_{sz}}$ which are the primary components of inertia force in *y* and *z* direction respectively. Since the forces are nonlinear, a sinusoidal random input describing function approach is being used [8].

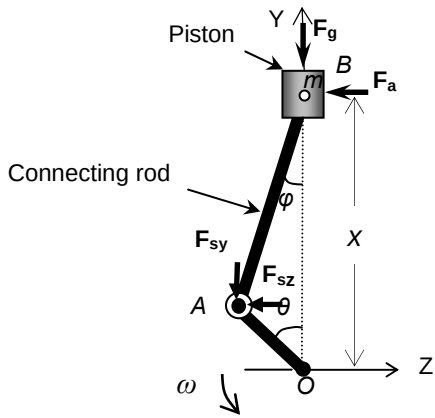

Figure 2.4 Single crank mechanisms

2.1.3 Modal Frequency Response

The equation of motion for a total system with harmonic excitation may be determined as

$$[\mathbf{M}]\{\ddot{\mathbf{q}}\} + [\mathbf{C}]\{\dot{\mathbf{q}}\} + [\mathbf{K}]\{\mathbf{q}\} = \{\mathbf{F}(\mathbf{t})\} \tag{13}$$

where $[\mathbf{M}], [\mathbf{C}]$ and $[\mathbf{K}]$ are the mass, damping and stiffness matrices respectively, and $\{\mathbf{F}(\mathbf{t})\}$ is the force. For harmonic excitations expressed in terms of frequencies, $\{\mathbf{F}(\mathbf{t})\} = \{\mathbf{f}(\boldsymbol{\omega})e^{i\omega t}\}$ and for harmonic motion, a harmonic solution in terms of modal coordinate $\{\xi(\omega)\}$ is assumed

$$\{\mathbf{q}\} = [\boldsymbol{\varphi}]\{\xi(\omega)e^{i\omega t}\} \tag{14}$$

$$\left[-\omega[\mathbf{P}]^{\mathrm{T}}[\mathbf{M}][\mathbf{P}] + i\omega[\mathbf{P}]^{\mathrm{T}}[\mathbf{C}][\mathbf{P}] + [\mathbf{P}]^{\mathrm{T}}[\mathbf{K}][\mathbf{P}]\right]\{\mathbf{x}(\boldsymbol{\omega})\} = [\mathbf{P}]^{\mathrm{T}}\{\mathbf{f}(\boldsymbol{\omega})\}$$

(15)

where

$[\mathbf{P}]^{\mathrm{T}}[\mathbf{M}][\mathbf{P}]$ – generalized mass matrix
$[\mathbf{P}]^{\mathrm{T}}[\mathbf{K}][\mathbf{P}]$ – generalized stiffness matrix
$[\mathbf{P}]^{\mathrm{T}}[\mathbf{C}][\mathbf{P}]$ – generalized damping matrix
$[\boldsymbol{\varphi}]^{\mathrm{T}}\{\mathbf{f}\}$ – modal force vector

For the case of modal damping, each mode has damping $\boldsymbol{c_i}$ where $\boldsymbol{c_i} = 2\boldsymbol{m_i}\omega_i\xi_i$. The equations remain uncoupled and represented in the form below for each mode.

$$-\omega^2\boldsymbol{m_i}\boldsymbol{x_i}(\omega) + i\omega\boldsymbol{c_i}\boldsymbol{x_i}(\omega) = \boldsymbol{f_i}(\omega) \tag{16}$$

Each of the modal responses is computed using

$$\boldsymbol{x}_i(\omega)=\frac{\boldsymbol{f}_i(\omega)}{-\boldsymbol{m}_i\omega^2+\boldsymbol{i}\boldsymbol{c}_i\omega+\boldsymbol{k}_i} \tag{17}$$

where $\boldsymbol{m}_i, \boldsymbol{c}_i, \boldsymbol{k}_i, \boldsymbol{x}_i$ and $\boldsymbol{f}_i(\omega)$ are the i^{th} mode modal mass, damping, stiffness, displacement and force.

2.1.4 Modal Assurance Criterion (MAC)

One of the developed techniques for quantifying the comparison between measured and predicted data mode shape is called *MAC*. *MAC* has been introduced as a measure of consistency and there is similarity between these two elements of two vectors. *MAC* is calculated in terms of a scalar quantity in the following equation;

$$MAC(r,q)=\frac{|\varnothing_r^T\varnothing_q^*|}{(\varnothing_r^T\varnothing_r^*)(\varnothing_q^T\varnothing_q^*)} \tag{18}$$

where the superscript T denotes the transpose and * denotes the complex conjugate. The data values $\varnothing_r$ and $\varnothing_q$ are the r^{th} and q^{th} columns of the real modal matrix ψ using the cross-product matrix which is

$\Omega = \varnothing^T \varnothing$

Thus, the *MAC* can be written as

$$MAC(r,q)=\frac{\Omega_{rq}^2}{\Omega_{rr}\Omega_{qq}} \tag{19}$$

The *MAC* value is expected to be close to 1.0 if the experimental and the theoretical mode shapes used are in fact from the same mode. Generally, it was found that the boundaries for acceptable (well correlated mode) and non correlation are quoted as above 80 per cent or less than 20 per cent, respectively.

2.1.5 Root Mean Square (RMS) And Power Spectral Density Function

In order to identify the energy transferred by an excited load case and to predict the energy distributions on the bearing journal, RMS values are calculated and the instructive knowledgeable results are obtained for the behaviours of the system.

2.1.6 Root Mean Square

The RMS value for a signal *f(t)* is defined as a square root of the mean value of quantity *f(t)* at a proper average time *T*. The RMS value is given by

$$\psi_s = \sqrt{\lim_{T \to \infty} \frac{1}{T} \int_{-T/2}^{T/2} f^2(t) dt} \tag{20}$$

ψ_s - signal directly related to energy.

2.1.6.1 Power Spectral Density Function

Auto-correlation function R_f offers information related to the characteristics of random variables in the time domain. The power

density function S_f offers similar information in the frequency domain.

$$R_f(\tau) = \lim_{T \to \infty} \frac{1}{T} \int_{-T/2}^{T/2} f(t) f(t+\tau) dt = \frac{1}{2\pi} \int_{-\infty}^{\infty} S_f(\omega) e^{t\omega\tau} \, d\omega \tag{21}$$

At the time domain, in the case of $\tau = 0$;

$$R_f(0) = \lim_{T \to \infty} \frac{1}{T} \int_{-T/2}^{T/2} f^2(t) dt = \psi_s^2 = \frac{1}{2\pi} \int_{-\infty}^{\infty} S_f(\omega) d\omega \tag{22}$$

It was clear that, the area under the frequency response curve in the frequency domain is equal to the RMS value at the time domain.

2.2.1 EXPERIMENT

For the experiment, the crankshaft was divided into 30 points, while impact hammer was in place, and the response of acceleration was measured. The crankshaft was supported on an approximately 90-mm thick sponge in order to allow it to be in a free-free end condition states for modal testing. Exciting the crankshaft with an impact hammer (5800A4 Dytran) at one point and measuring the responses at all 30 measuring points using an accelerometer (3100B Dytran), allowed the transfer function of the crankshaft to be obtained by means of an FFT(fast Fourier analyser(SA-390). Figure 2.5 shows the experimental set-up and the measurement system.

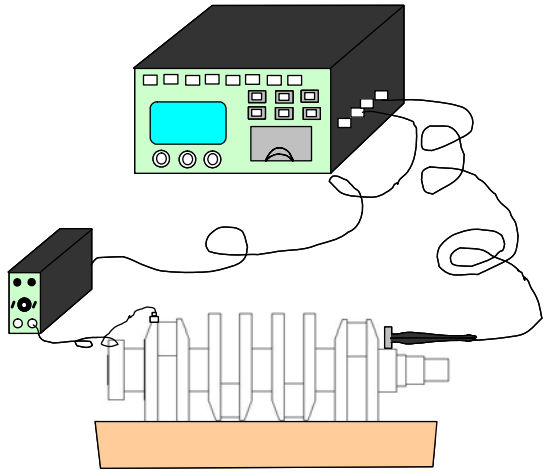

Figure 2.5 Experimental set-up and measurement system

2.2.2 RESULTS

2.2.3 Verification Frequency Response, Natural Frequencies, Mode Shapes and MAC Properties

By exciting the crankshaft with an impact hammer at one impact point and measuring the responses at all of the points, the transfer function of the crankshaft is obtained by means of the FFT analyser and some signal processing. Two spectra cases of frequency responses from this crankshaft for experiment and simulation are shown in the Figures 2.6 (a) and (b). Figure 2.6(a) is a response in the in-plane case and the Figure 2.6 (b) is the out-plane case. From the spectra, the natural frequencies of the first 10 modes under 2000 Hz occur for four in-plane modes at 312.8 Hz,

725.5 Hz, 1007.1 Hz and 1615.4 Hz and six out-plane at 364.3 Hz, 824.4 Hz, 1133.5 Hz, 1362.7 Hz, 1814.1 Hz, and 1981.3 Hz, and correspond to each of the peaks shown in Figure 2.6(a) and (b) respectively. In order to verify these results, theoretical modelling was performed and the results were compared. Table 1 shows a comparison of the natural frequencies between theoretical and experimental results. The percentages of relative errors are very small except for mode 2 (first out-plane mode). This is because of the rigidity of the crankshaft itself and the complexity of the structure, especially at the overlap between the journal and the pin crank, which provides a thickness at the overlap section that influences the natural frequency. However, the mode can still be categorized into their prevailing vibration, which is a bending vibration. Figures 2.7 (a) and (b) show the mode shape comparison between experiments and computer simulation for both in-plane and out-plane modes.

Table 1.1 Comparison of natural frequency between experiment and computer simulation

Mode No	simulation (Hz)	Experiment (Hz)	MAC value
(1,1)	312.8	335	0.931
(2,2)	364.3	460	0.981
(3,3)	725.5	750	0.881
(4,4)	824.4	805	0.902
(5,5)	1007.1	1080	0.811
(6,6)	1133.5	1215	0.868
(7,7)	1362.7	1415	0.833
(8,8)	1615.4	1610	0.879
(9,9)	1814.1	1865	0.868
(10,10)	1981.3	1970	0.811

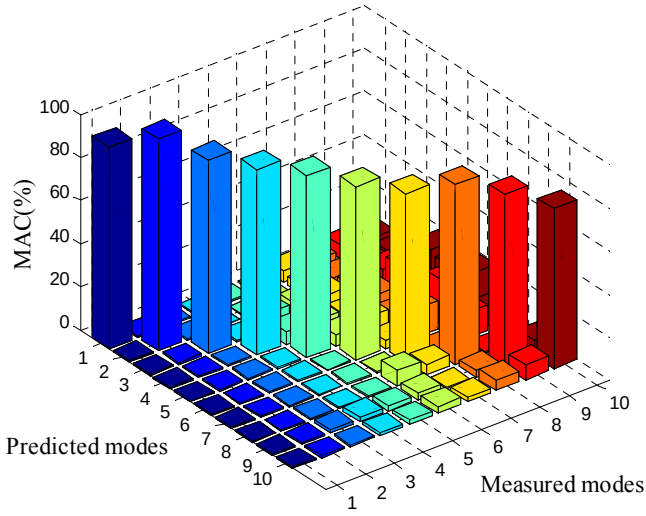

Figure 2.6 Graphical presentations of MAC properties

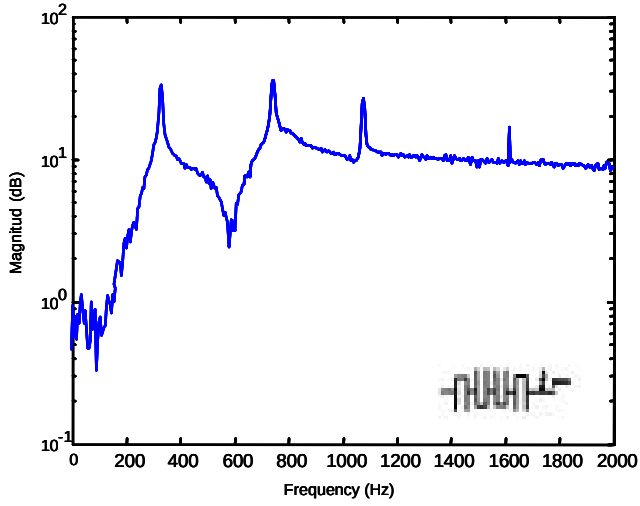

i. Experiment
(a)

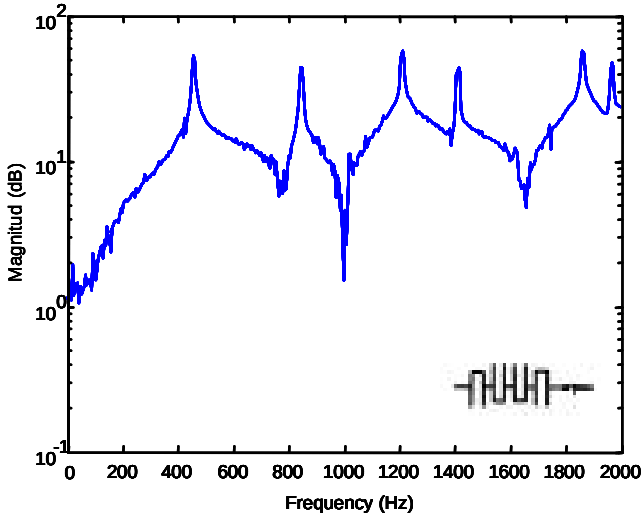

i. Experiment

(b)

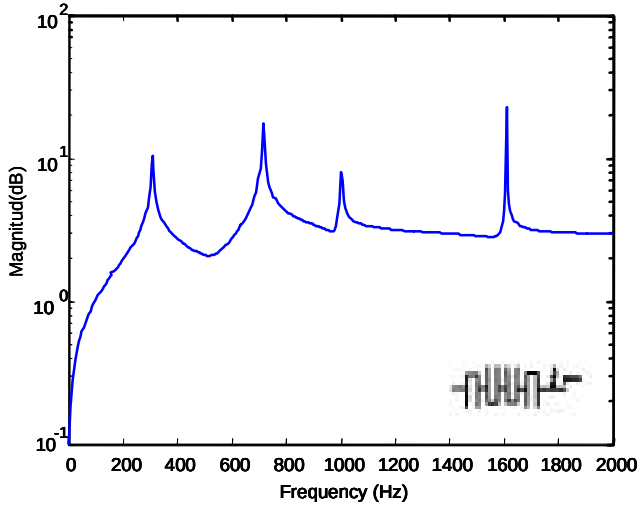

ii simulation

(a)

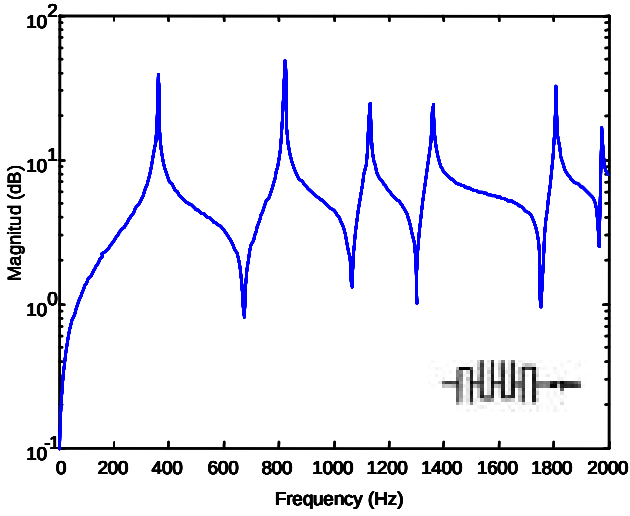

ii. simulation
(b)

Figure 2.7 Comparison of frequency response between experimental and computer simulations for (a) the in-plane frequency response (b) the out-plane frequency response

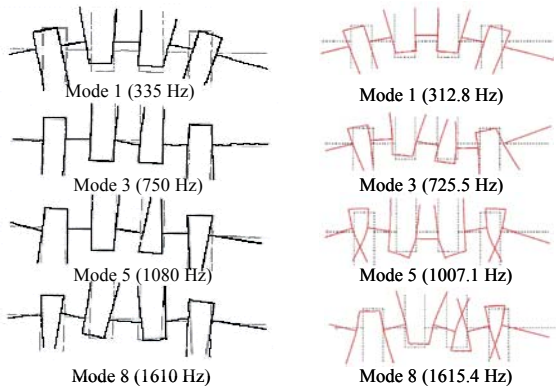

(a)

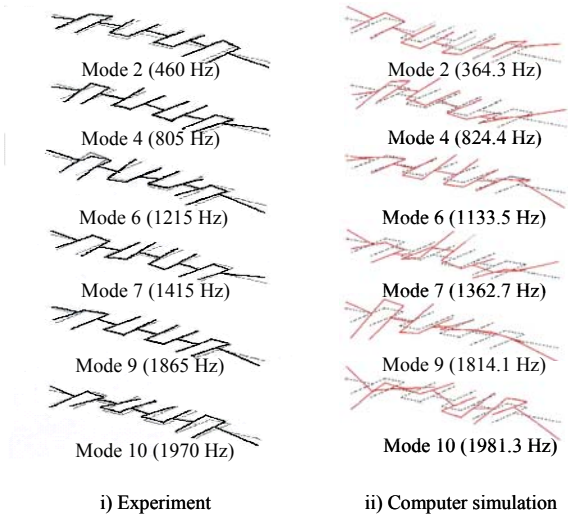

(b)

Figure 2.8 Comparison of mode shapes between experimental and computer simulations for (a) the in-plane and (b) the out-plane mode

2.2.4 Firing Load Cases Response

After the modelling had been verified, the crankshaft was idealised with applicable engine model systems. The forces acting on the firing condition were investigated and the characteristics of the responses identifying the load cases 3 and 1 and load cases 3 and 2 were compared and measured. Table 2 gives the description of the load case; three types of load case were considered.

Firstly, the force acting on the firing condition was investigated. Normally, the forces are expanded into a series of harmonic force components by Fourier analysis in time domain, but, since the forces are nonlinear, a sinusoidal random input function was used. Next, from Figures 2.8 (a) and (b), it can be seen that for load case 3, in the vertical and lateral directions, the exciting response is

comparably higher than for load case 1 in the vertical direction. Load case 3 also maintained a higher level response than load case 2. Therefore, to identify the average response excited at each bearing journal, only load case 3 was selected to be used for the next analysis.

Table 1.2 Load cases

Type	Description
Load case 1	vertical direction
Load case 2	lateral direction
Load case 3	vertical and lateral direction

2.2.4.1 RMS Value at the Bearing Journals

Based on the above results, the average excited load response at the bearing journals was identified using the RMS values. The RMS value is very simple and makes it easier to identify the average of energy transferred at a certain given load. The highest RMS values provide the highest energy, but the disadvantage of this energy is that it can reduces the lubrication film thickness in the bearing journal and causes wear. Figure 2.9 shows the level of RMS values for each bearing journal at the crankshaft. The location of bearing journal 2 was identified as having the highest energy calculated using RMS value. The RMS value decreased linearly until the energy at bearing journal 5 was calculated. The highest RMS value at bearing journal 2 occurred because of the effects of alternating energy donated by the flywheel located at the left-hand side which created a bending mode shape.

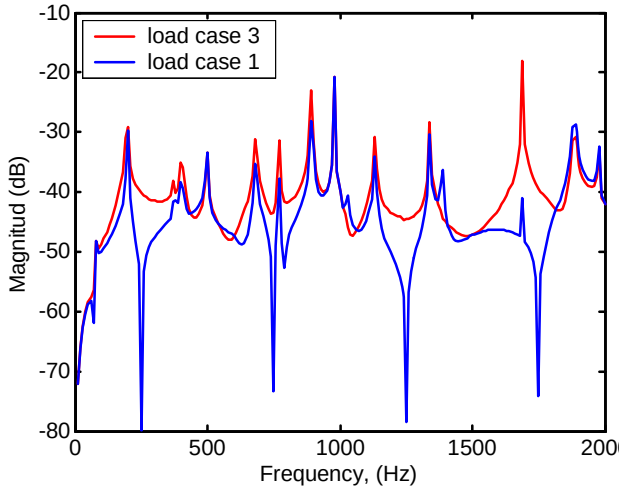

(a)

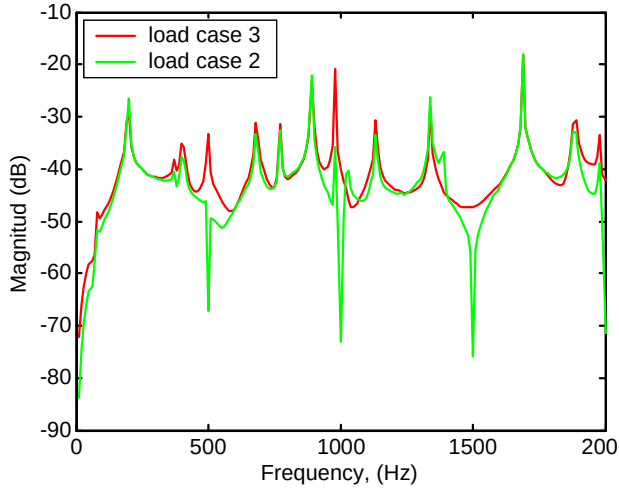

(b)

Figure 2.9 Comparison of responses between (a) load cases 3 and 1(exciting at the first crank pin) and (b) load cases 2 and 3 (exciting at the first crank pin)

2.2.4.2 Effects of the Counter Weight Modification

The crankshaft could not be modified easily, and moreover the experimental approach with a new modification structure in the crankshaft would be very expensive to implement and time consuming. To overcome this problem, a theoretical approach was used, which required considerably less time and cost to predict the behaviour of the crankshaft system faster and easier through the energy stored in the shaft system. Ideally, the crankshaft counter weights are given a step by step modification in the same way as the additive stiffness process shown in Figure 2.10. The responses due to this counter weights modification are measured at each step on bearing journal 2. The RMS values were calculated to identify the transferable energy and the lowest RMS value was used to provide the suitable shape for the crankshaft counter weights. Figure 2.11 shows the levels of RMS values for each case, with a modification for three repeatable counter weights. It was found that modification of the counter weight could give beneficial effects to the energy characteristics and transferable energy at a level of RMS value that decreased linearly. As a result, the shape of the optimum counter weights was found from the lowest RMS value.

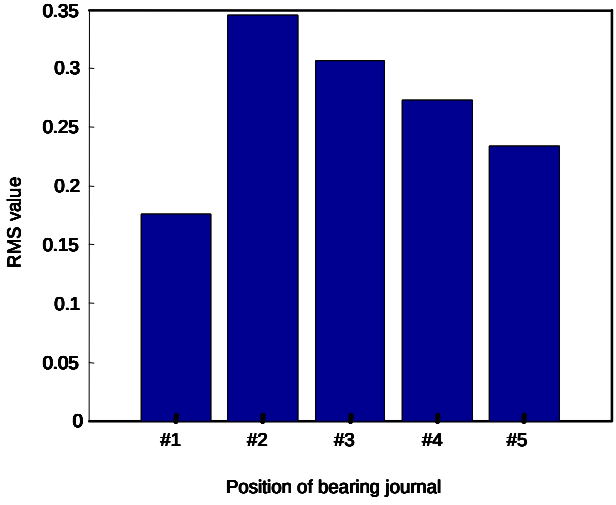

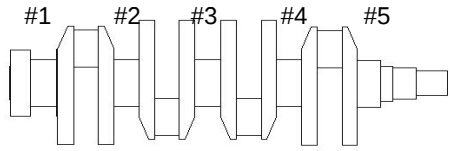

Figure 2.10 Comparison of the RMS values at each bearing journal

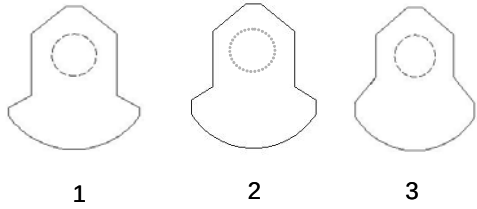

Figure 2.11 Counter weight modeling (1-original)

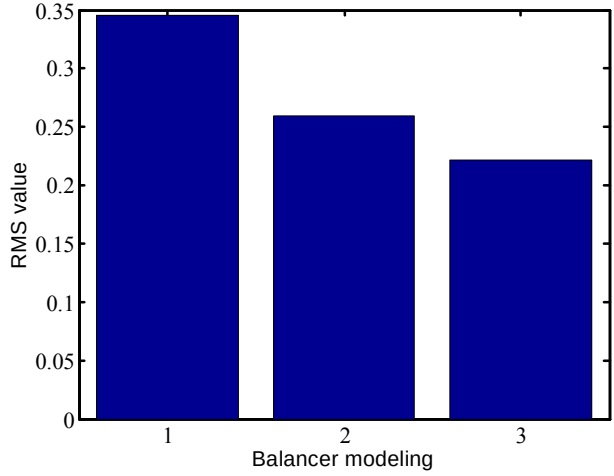

Figure 2.12 Comparison of the RMS value corresponding to the counter weight shape

2.3.1 CONCLUSION

The crankshaft for an automotive internal combustion inline engine was investigated and the conclusion is drawn as follows:

1. The in-plane and out-plane natural frequencies, mode shapes, frequency responses and MAC values are in good agreement with the experimental results. Thus, the modelling of the crankshaft was verified.
2. The characteristics of a load case were identified by using both vertical and lateral directions forces. It was verified that the vertical force gave a higher load.
3. The RMS value was found to be a simple method in identifying the energy transfer in vibration which was dominantly excited at bearing journal 2.
4. The modification to the counter weight produced lower RMS values and it was easy to reach an optimum design of crankshaft counter weights.

REFERENCES

1 Kang, Y., Sheen, G. J. and Tseng, S. H. 1998, Modal Analyses and Experiments for Engine Crankshafts, *Journal of Sound and Vibration*, ,214(3): 413-430

2 Lee, J. Y., Aminudin, and Oh, J. E. 2003. *The Three-Dimensional Crankshaft Analysis using Transfer Matrix Method*. Proc. Of Malaysian Science an Technology Congress, Cititel, Midvalley, Kuala Lumpur, Malaysia

3 Kim, K. S, Oh, J. E., Lee, J. Y., and Kim, M. B**.** 1991. Two Dimensional Vibration Crankshaft Analysis Using Transfer Matrix, *KSME*, Vol. 15, No. 2: 55~462,

4 Morita T. and Okamura H. 1995. Simple Modeling and Analysis for Crankshaft Three-Dimensional Vibrations, Part 2: Application to an Operating Engine Crankshaft, *Trans. of the ASME*, vol. 117: 80-86.

5 Tetsuji, M. and Hideo, M., Analysis of Crankshaft Three-Dimensional Vibrations in a Rotating Coordinate System, *SAE 951292*: 473 – 480

6 Okamura H., Shinno A., Yamanaka T., Suzuki A., and Sogabe K.1995. Simple Modeling and Analyses for Crankshaft Three-Dimensional Vibration, Part I: Background and Application to Free Vibrations, *Trans. of the ASME*, vol. 117:70-79.

7 Khang, U J.1991. *Eigenmode Sensitivity and Structure Modification for Improvement of Dynamic Characteristics of Engine Mount System,* Ms Thesis, Department of Precision Mechanical Engineering, Hanyang University.

8 Rao V. D. 2000. *Vehicle Dynamics*, Narosa Publishing House, India

9 Kazuomi, O. and Mitsuo N.1980. Relation Between Crankshaft Torsional Vibration and Engine Noise, *SAE* 790365:1291-1298

10 Martin, S., Frank, K, Herald, S. and Rolf I. 2000.*Combustion Supervision by Evaluating the Crankshaft Speed and Acceleration*, SAE 2000 World Congress, 2000-01-0558: 1-8

11 Mourelatos Z. P**.** 2000. An Efficient Crankshaft Dynamic Analysis Using Substructuring With Ritz Vectors*, Journal of Sound and Vibration*, 238(3): 495 -527

12 MSC/NASTRAN *User's Manual*, 2001. Volume 1 & II The MacNeal Schwendler Corp. Los Angeles, California